Nuclear Cross Sections for Negative Pions of Energy 113 and 137 Mev*

RONALD L. MARTIN†
Institute for Nuclear Studies, University of Chicago, Chicago, Illinois
(Received May 26, 1952)

The measurements of the nuclear cross sections for negative pions at 85 Mev, recently made by Chedester, Isaacs, Sachs, and Steinberger, have been extended to 113 and 137 Mev. The total absorption plus inelastic scattering cross sections were obtained from a transmission measurement in poor geometry. The cross sections are all close to the geometrical value, $\pi A^{2/3}(\hbar/\mu c)^2$, within the accuracy (15 percent) of this technique. With the possible exception of carbon there is no evident energy dependence in the range 85 to 137 Mev.

AMONG mesons, the pi-mesons are distinguished by their strong nuclear interaction. With the availability from the large synchrocyclotrons of fairly intensive π^- meson (pion) beams well collimated and well defined in energy, it has become possible to make accurate measurements of the nuclear cross sections of pions as a function of energy. Using one of the pion beams of the Nevis cyclotron, Chedester, Isaacs, Sachs, and Steinberger[1] have obtained the absorption cross sections of various nuclei at 85 Mev by transmission measurements in poor geometry using scintillation counter techniques. Except for hydrogen, the cross sections which they obtained were close to the "geometrical value" $\pi A^{2/3}(\hbar/\mu c)^2$. A is the mass number and $\hbar/\mu c = 1.4\times10^{-13}$ cm is the range of nuclear interaction. Studies of negative pions in the energy range 30 to 110 Mev in photographic emulsions by Bernardini, Booth, and Lederman[2] showed that while the cross section for absorption and inelastic scattering for the nuclei in these emulsions is close to the geometrical value, there is some indication of a decrease in cross section with decreasing pion energy.

This paper reports an extension of the measurements of Chedester, Isaacs, Sachs, and Steinberger by essentially the same technique, using negative pions of energies 113 and 137 Mev. A preliminary report has already been made to this journal.[3]

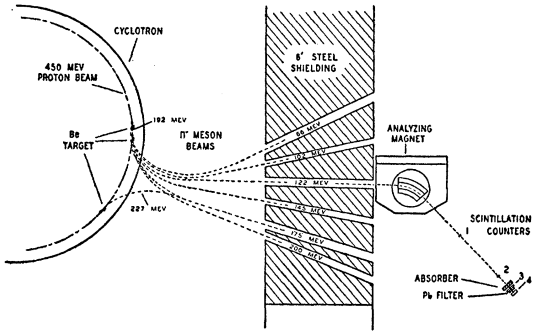

FIG. 1. Experimental arrangement.

THE PION BEAMS

Pions are produced by the bombardment of either beryllium or copper targets with the internal 450-Mev proton beam of the Chicago synchrocyclotron. Negative pions emitted in the forward direction are deflected outward by the magnetic field of the cyclotron and emerge from the vacuum chamber through a thin aluminum window. The cyclotron field separates the pions according to their energy by deflecting those of lower energy more; those of higher energy less. A certain amount of focusing takes place in the fringing field of the cyclotron such that a sizeable fraction of the mesons of given momentum leave the cyclotron in a fairly parallel beam. Channels were cut in the six-foot steel shield which separates the cyclotron from the experimental room so that a number of these beams having different energies are able to enter the experimental room.

The location of these channels was obtained from an empirical study of the meson trajectories using the current carrying wire method.[4] This method depends on the fact that if a given tension T is applied to a thin wire with current I in a transverse magnetic field $H_z(xy)$, the wire will contort itself into precisely the same horizontal trajectory as will be followed by a particle of charge e and momentum

$$P=(e/c)(T/I). \quad (1)$$

One end of the wire was fixed at the position of the target in the median plane of the cyclotron. The other end was brought into the experimental room, passed over a pulley, and attached to a weight so as to apply a known tension. The current in the wire was then adjusted until the wire remained in stable equilibrium. In this way channels were laid out corresponding to pion energies, calculated using (1), of 66, 102, 122, 145, 175, and 200 Mev. The target position to which these energies refer is 76-in. radius and 3.8° NE azimuth. The channels were all 2 in. high, some were 4 in. wide and others 6 in. wide. The general arrangement is shown in Fig. 1.

Since much stray radiation, mostly fast neutrons, come through the channel from the cyclotron, it was found expedient to use a magnet to deflect the pions

* Research sponsored by the ONR and AEC.
† AEC Predoctoral Fellow.
[1] Chedester, Isaacs, Sachs, and Steinberger, Phys. Rev. 82, 958 (1951).
[2] Bernardini, Booth, and Lederman, Phys. Rev. 83, 1075 (1951).
[3] Martin, Anderson, and Yodh, Phys. Rev. 85, 486 (1952).
[4] J. J. Thomson, Phil. Mag., Series 6, 13, 561 (1907).

through an angle of about 45° so as to obtain a purified beam of the desired particles. Muons and electrons having the same sign and momentum as the pions remain in the deflected beam. For the 122- and 145-Mev beams used in the present experiment these were found to amount to 7±4 percent of the pion intensity. The deflecting magnet has a focal length of 21 in. in the horizontal direction and so provides some focusing.

Positive pions up to 145 Mev have been obtained by reversing the direction of both the cyclotron and the deflecting magnet fields. Positive pions emitted in the direction backward from the proton beam (now reversed) follow the same trajectories and pass through the same channels as did their negative counterparts of the same energy. The number of positive pions obtained in this way is much smaller than the number of negatives, backward emission being far less favorable for the pions. In the experiments described herein only the 122-Mev and 145-Mev negative pion beams have been utilized.

EXPERIMENTAL ARRANGEMENT

The pions were detected by means of scintillation counters. Four such counters were arranged in the line of the pion beam. The first pair were 1 inch square by 1 cm thick terphenyl crystals spaced either 30.5 in. or 40 in. apart. The second pair were liquid scintillators having an effective diameter of 3 in. placed together and removed either 9.15 in. or 19.9 in. from the second crystal. The latter distances refer to a point 1 cm inside the last scintillator.

Coincidence circuits were arranged to record the quadruple coincidence produced when an ionizing particle penetrated all four scintillators, and also the double coincidence when the particle traversed the first pair. Thus, the ratio (Q/D) of quadruples to doubles is the fraction of particles which penetrate the last pair of scintillators after having passed through the first pair. An absorber placed in front of the second pair of scintillators removes pions from the beam with the result that the ratio quadruples to doubles is reduced. Comparison of this ratio with and without absorber is expressed as a cross section by means of the formula

$$Q/D \text{ with absorber}/Q/D \text{ without absorber} = \exp(-N\sigma), \quad (2)$$

where N is the number of atoms per cm^2 in the absorber and σ is the cross section in cm^2. Some amount of correction of the ratios Q/D was necessary to account for the effects of chance coincidences.

The last pair of scintillators were made purposefully large, and the absorbers left as close to them as possible so that the cross section measured in this way would not include much of the effects of Coulomb scattering and small angle diffraction scattering. A $\frac{1}{16}$ in. thick lead absorber was placed between the last two scintillators to render them insensitive to those protons of energy less than 100 Mev which might be emitted from the stars produced by the absorption of pions. The scintillators were rather insensitive to neutrons and gamma-rays which might come from such stars. The cross sections obtained in this way are primarily total cross sections for the absorption and inelastic scattering of pions.

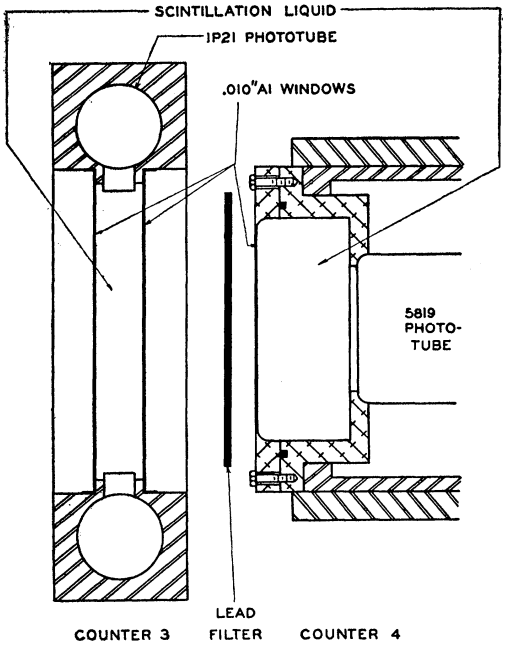

FIG. 2. Detail of counters No. 3 and No. 4. In use the two counters were fitted tightly together.

SCINTILLATION COUNTERS

The first two scintillators were 1 in.×1 in.×1 cm thick crystals of *p*-terphenyl of good optical quality. These were mounted using a thin layer of silicone grease to provide good optical contact between one edge of the crystal and the flat photo cathode of the EMI 5311 photomultiplier. The crystal was wrapped in thin aluminum foil to improve the optical efficiency. Photomultiplier and crystal were mounted together inside a $\frac{3}{8}$ in. thick steel cylinder which served as a magnetic shield. Openings $1\frac{1}{2}$ in.×$1\frac{1}{2}$ in. were cut in the shield opposite the crystal faces to allow for the uninterrupted passage of pions through the crystal. These openings were made light tight by a wrapping of black Scotch electric tape.

Scintillator No. 3 was of the liquid transmission type 4 in. in diameter and $\frac{5}{8}$ in. thick. The cell was machined out of a single block of low carbon steel and provided with 0.010-in. aluminum windows sealed in place with Araldite 101 cold setting adhesive. The scintillator liquid was viewed edge-on by two diametrically opposite 1P21 photomultiplier tubes set in cavities bored in the sides of the steel cell. The glass envelopes of these tubes was sealed to the steel with Araldite 101 adhesive so that the liquid scintillator was in direct optical contact with the glass window of the phototube. The liquid

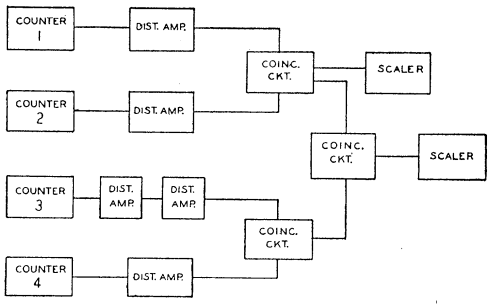

FIG. 3. Block diagram of counting arrangement.

scintillator was the 3 grams per liter mixture of terphenyl in phenylcyclohexane recommended by Kallman and Furst.[5] A sketch of the design is given in Fig. 2.

Scintillator No. 4 was an end-on type using the same type of liquid as scintillator No. 3. The scintillation cell was machined from aluminum and was 3 in. in diameter and $1\frac{1}{4}$ in. deep. This cell was viewed by a 5819 photomultiplier mounted on its central axis. The photocathode was sealed to the cell with Araldite No. 101 adhesive so that it made direct optical contact with the scintillation liquid. The design of this scintillator is also shown in Fig. 2.

The outputs of the photomultiplier tubes were fed directly into RG7U (95-ohm) cable which carried the pulses some 150 feet to the cyclotron control room. There they were amplified using 100-ohm distributed amplifiers[6] having a 3×10^{-9} second rise time and thence fed into the coincidence circuits. A gain of 100 was needed for scintillator No. 3; for the others a gain of 10 sufficed. A block diagram of the counting arrangement is shown in Fig. 3. The coincidence circuits were fashioned after that described by Garwin.[7] The resolving time of these circuits was about 5×10^{-8} second. It was necessary to lengthen the pulses from the photomultipliers to about this time in order to obtain satisfactory operation. Diode pulse lengtheners were used to accomplish this. One coincidence circuit operated from pulses of the first pair of scintillators and a second coincidence circuit operated from the pulses of the second pair. The quadruple coincidences were obtained by recording from a third and slower circuit the coincidence of the output pulses from the two primary coincidence circuits. Hewlett Packard fast decade scalers with a resolving time of 0.1μ sec made it possible to count as rapidly as 100,000 counts per minute without appreciable loss.

The pulses obtained from the scintillators were not uniform in height due to variation of optical efficiency over the sensitive area. However it was possible to count mesons with nearly 100 percent efficiency by using a sufficiently high voltage on the photomultipliers. Curves of coincidence counting rate in the meson beam as a function of photomultiplier high voltage were taken and showed satisfactory plateaus. A typical plateau curve is given in Fig. 4.

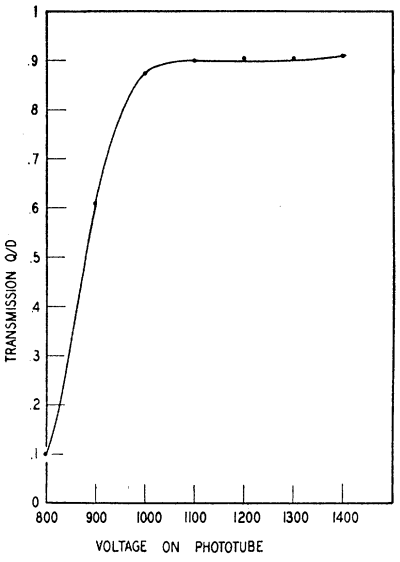

FIG. 4. Plateau curve of counter No. 4.

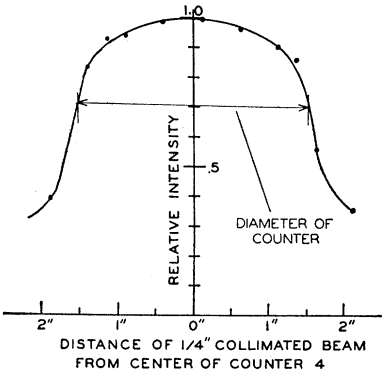

FIG. 5. Sensitivity of counter No. 4.

A study of the effective area of the second pair of scintillators was also made. For this a $\frac{1}{4}$-in. hole was bored in a 4 in. thick lead brick set in the meson beam. The counting rate of counters No. 3 and No. 4 was measured with various parts of their area exposed to this narrow pencil of mesons. The counting efficiency was found to be fairly uniform over most of the 3-in. diameter area of counter No. 4 as shown in Fig. 5.

TARGET

Beryllium was used as the meson-producing target of the cyclotron in the experiments with the 122-Mev beam, and copper in the experiments with the 145-Mev beam. The target is provided with a thermocouple arranged to monitor rather accurately the meson output of the machine. The target is connected through a calibrated heat leak to a large cylindrical drum, capable of

[5] H. Kallman and M. Furst, Nucleonics **8**, 32 (1951).
[6] Anderson, Martin, and Slattery, Rev. Sci. Instr. (to be published).
[7] R. L. Garwin, Rev. Sci. Instr. **21**, 569 (1950).

maintaining itself at a fairly constant temperature by radiation. The thermocouple junctions are connected across the heat leak so that the emf developed is a function of the heat flow through the leak. This emf is recorded on a Brown potentiometer and read as watts of power developed by the proton beam in the target. The proton beam loses energy to the target principally by ionization loss and to some extent by nuclear reaction, but in any case the energy loss is proportional to the path length of protons in the target and hence to the meson output. The thermocouple data are not an essential part of the measurements described here, but they have been useful as an over-all check on the operation of the equipment. Throughout these experiments the doubles count per target watt minute was computed. The constancy of this number for given geometry was taken as an indication that the equipment was operating reproducibly and reliably.

DEFLECTION MAGNET

A 45° sector magnet with a gap 2 in. high and 4 in. wide was used to deflect the mesons and separate them from undesirable radiation which comes through the channel in the shield. The current in the magnet was adjusted to give a maximum in the doubles rate of counters No. 1 and No. 2. Typical curves of this counting rate as a function of magnet current are given in Fig. 6. The width of these curves is due partly to the energy spread of the beams (±4 Mev) and partly from the finite extension of the channel openings and the scintillation detectors. The curves for the 122-Mev and the 145-Mev beams are not strictly comparable. The former were taken with a 40-in. spacing between the counters, the latter with 30.5-in. spacing. The intensity of the 122-Mev π^- beam was found to be some 7 times greater than that of the 145-Mev beam. This is due to the more abundant emission of the lower energy mesons and to the focusing properties of the cyclotron fringing field, which seems to be most efficient for the 122-Mev beam.

Some idea of the background level in the experimental room is given by the fact that with the magnet current turned off the singles rate of counter No. 1 was reduced to 5 percent of its value with the magnet current properly adjusted for the 122-Mev beam. The number of collimated particles capable of producing a double coincidence in counters No. 1 and No. 2 was negligible with the magnet turned off.

ENERGY AND COMPOSITION OF THE BEAMS

Wire measurements were made to establish the momentum of the particles accepted by the deflection magnet. These were made with the wire (No. 32 copper) fixed at the center of the channel on the cyclotron side and passing through the center of the channel, the slot in the deflecting magnet, and along the centerline of the scintillation counters, where it was fastened to a trip balance specially adapted to measure the horizontal

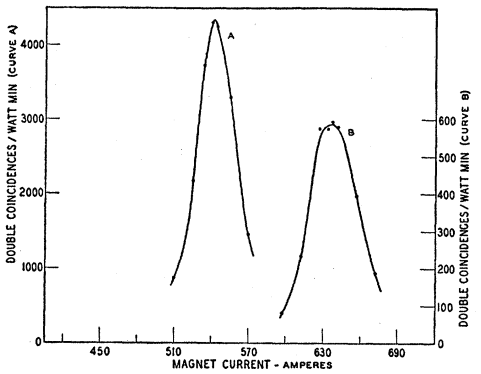

FIG. 6. Intensity *vs* deflecting magnet current.

tension in the wire directly in grams. The current in the wire was determined from a measurement, with a precision potentiometer, of the voltage it developed across a standard 0.1-ohm shunt. In the 122-Mev channel with the magnet current at the value which gave maximum beam intensity the following readings were obtained:

Tension (grams)	Current (amperes)	Momentum (units of μc)
106.2	1.4002	1.583
122.2	1.6145	1.578

This corresponds to an energy of 122.7 Mev for pions of mass $\mu = 276$ electron masses.

The range was measured by making transmission measurements with various thicknesses of aluminum. The transmissions obtained in this way are plotted on a logarithmic scale in Fig. 7. There are two sharp drops. The first occurs at the end of the pion range, the second at the end of the range of the muons which contaminate the beams. Without corrections the mean ranges in the 122-Mev beam are 42.2 g/cm² and 60.5 g/cm² of

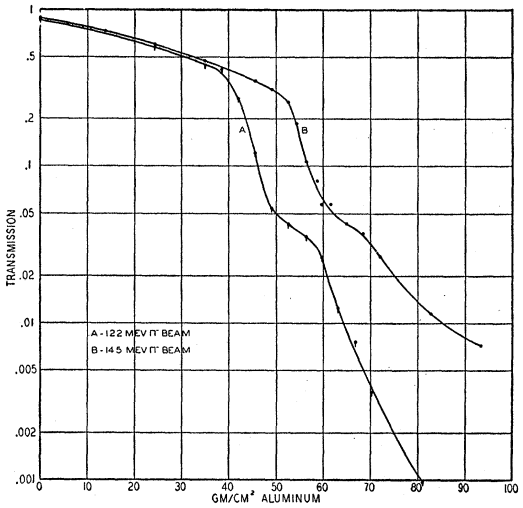

FIG. 7. Range curves in aluminum of 122-Mev and 145-Mev π^- beams.

TABLE I. Absorber data.

Absorber	Thickness (cm)	g/cm²	N (10^{23} atoms/cm²)	X_n[a] (cm)
C_1	3.33	5.202	2.609	4.43
C_2	6.50	10.231	5.131	6.01
Al_1	2.50	6.978	1.558	4.01
Al_2	5.00	13.965	3.119	5.26
Cu_1	1.00	8.931	0.846	3.24
Cu_2	2.00	17.764	1.683	3.76
Cd_1	1.27	10.963	0.587	3.40
Sn_1	1.27	9.281	0.471	3.40
Pb_1	1.20	13.608	0.3955	3.36
Pb_2	2.40	27.333	0.7945	3.96

[a] X_n is the distance from the center of the absorber to a point 1 cm inside the last scintillator.

aluminum. Other materials in the beam contribute 6.4 g/cm² aluminum equivalent as follows:

Material	Al equivalent g/cm²
Counters No. 1 and No. 2	3.0
Liquid of counter No. 3	2.0
Aluminum windows	0.2
1 cm of liquid of counter No. 4	1.2
Total aluminum equivalent	6.4 g/cm²

The energies were computed using the tables of proton ranges given by Smith,[8] taking as mass ratios, 6.65 for the proton to pion and 8.76 for the proton to muon. From the above data the energy of the primary pions in the 122-Mev channel was found to be 128 Mev; of the primary muons 150 Mev.

In the 145-Mev channel the wire measurements gave for the momentum the value 1.78μc. The corresponding pion energy is 147 Mev. The range measurement gave 150 Mev for the pions and 167 Mev for the muons.

The pion energy obtained from the range measurement is slightly higher than that expected on the basis of the wire measurement in both channels. Some of this discrepancy is due to the way in which the range is measured. Negative pions that come to rest at the end of their range produce stars, the particles of which are able to penetrate an additional amount of absorber and produce a pulse in the final scintillators. In addition, the energy of the pions in a given channel depends on the position of the target and on the value of the cyclotron magnetic field and these are not always precisely reproduced.

For the purposes of the cross-section measurements the pertinent energy is the mean energy of the pions traversing the absorber. This was slightly different for the different absorbers used. Taking into account the energy loss in the first two scintillators the energy of the pions entering the absorbers, which was adopted on the basis of the studies described above, was 120±4 Mev for the 122-Mev channel and 143±4 Mev for the 145-Mev channel.

The muons have very nearly the same momentum as the pions and come partly from the vicinity of the target, from which they follow the same trajectory as the pions, and partly from the decay in flight of the pions in the beam. Their number may be estimated from the range curve and amounts to about 7 percent in both beams. The residual particles giving rise to the tail of the range curves were either neutrons from pion-produced stars or electrons. In the 122-Mev beam the electron content was less than 1 percent of the beam intensity while in the 145-Mev beam the electron content was somewhat larger because the cyclotron target for this beam was copper. In both cases the electron content was included in the estimate of the muon contamination so that the total beam contamination was 7±4 percent in both beams.

BACKGROUND

In the experiment, the principal source of background was the chance coincidence count due to the high beam intensity and the finite resolution of the coincidence circuits. The effect is aggravated by the pulsed operation of the cyclotron. The duty cycle of the cyclotron is about 1 percent so that the instantaneous counting rate is 100 times the average counting rate. The chance coincidence rate is proportional to the square of the beam intensity and to the ratio of the resolving time τ of the coincidence circuit and the duty cycle D of the cyclotron. The ratio τ/D was determined by exposing the counters to two different pion beams at the same time so that all coincidences were chance coincidences. The values found were 2.5×10^{-6} second for the doubles coincidence circuit of counters No. 1 and No. 2, and 1.0×10^{-4} second for the quadruples coincidence circuit.

TABLE II. Data of the 122-Mev π^- beam.

Abs.	Mean energy / Energy band Mev	Doubles count	Quad. count	Q/D	Q/D[a]	σ 10^{-27} cm² (experimental)
No abs.		153030	136695	0.8933 ±0.0011	0.8861	
C_1	114 105–124	160033	131821	0.8237 ±0.0015	0.8028	404 ±37
No abs.		147300	132558	0.8999 ±0.0031	0.8930	
Al_1	114 105–124	184786	152575	0.8257 ±0.0036	0.8118	655 ±54
No abs.		133520	120905	0.9055 ±0.0013	0.8988	
Cu_1	112 101–124	129788	109101	0.8407 ±0.0012	0.8281	1037 ±67
No abs.		136172	122842	0.9021 ±0.0022	0.8952	
Cd_1	112 100–124	130001	108241	0.8326 ±0.0014	0.8174	1659 ±127
No abs.		144637	130008	0.8989 ±0.0011	0.8913	
Sn_1	114 104–124	150263	126728	0.8434 ±0.0021	0.8279	1680 ±144
No abs.		144533	129974	0.8993 ±0.0016	0.8916	
Pb_1	111 98–124	144122	118861	0.8247 ±0.0017	0.8078	2668 ±208

[a] Corrected for background.

[8] J. H. Smith, Phys. Rev. **71**, 32 (1947).

The energy delivered to the target was used as an indication of the cyclotron operating level. At various times the singles counting rates S_1 and S_2 of counters No. 1 and No. 2 were recorded and also the doubles rate D_{34} of counters No. 3 and No. 4. With these data it was possible to distinguish the random from the true count. The backgrounds (bg) were computed using the formulas

$$\frac{D_{12}(\text{bg})}{\text{min}}=\frac{2.5\times10^{-6}}{60}\left(\frac{S_1}{\text{watt min}}-\frac{D_{12}}{\text{watt min}}\right)\times\left(\frac{S_2}{\text{watt min}}-\frac{D_{12}}{\text{watt min}}\right)\times\text{watts}^2, \tag{3}$$

$$\frac{Q(\text{bg})}{\text{min}}=\frac{1.0\times10^{-4}}{60}\left(\frac{D_{12}}{\text{watt min}}-\frac{Q}{\text{watt min}}\right)\times\left(\frac{D_{34}}{\text{watt min}}-\frac{Q}{\text{watt min}}\right)\times\text{watts}^2. \tag{4}$$

In the 145-Mev beam the backgrounds were about 0.3 percent of both the doubles and the quadruples count with the cyclotron operating at a 5-watt level. In the more intense 122-Mev beam the backgrounds were about 1 percent of the doubles count and 3 percent of the quadruples count with the cyclotron operating at a 12-watt level. The net effect of the background on the cross section was about 1.5 percent in the 145-Mev beam and 12 percent in the 122-Mev beam.

MEASUREMENTS

The transmission measurements were made in "poor" geometry with the absorber as close to counter No. 3 as possible. A list of the absorbers used, together with pertinent data about them is given in Table I. The thickness of the absorber was severely limited by the requirement that the effect of multiple Coulomb scattering should be kept small. Estimates of the magnitude of this effect were made using a simplified theory of the multiple scattering.[9] These effects were negligible for the 5.2-g/cm² graphite absorber and range to 7.5 percent in the worst case, 13.6-g/cm² of lead in the 122-Mev beam. These corrections would become very much greater if the absorbers were placed further from the last pair of counters. Such a geometry also precludes the measurement of pions scattered in the forward direction by nuclear interaction. The solid angle subtended by the fourth counter at the center of the absorber was of the order of 3.8 steradians. Thus, the cross sections which are obtained experimentally do not include processes in which ionizing particles are produced within this solid angle and which have sufficient penetrating power to traverse the last pair of scintillators. For the most part, these are the elastically diffracted pions. Estimates made by applying the theory of diffraction scattering show that all except 6 percent of the elastically scattered pions in the most favorable case (lead), and all except 20 percent in the worst case (carbon) enter the final pair of counters. Thus, these experiments measure primarily the total cross section for the nuclear absorption of the pions.

[9] B. Rossi and K. Greisen, Revs. Modern Phys. **13**, 240 (1941).

TABLE III. Data of the 145-Mev π^- beam.

Abs.	Mean energy / Energy band Mev	Doubles count	Quad. count	Q/D	Q/D[a]	σ 10^{-27} cm² (experimental)
No abs.		7704	7081	0.9191 ±0.0051	0.9155	
C_1	138 128–147	23632	19565	0.8279 ±0.0038	0.8276	414 ±27
No abs.		13641	11541	0.8461 ±0.0031	0.8461	
C_2	133 118–147	12284	8249	0.6715 ±0.0064	0.6694	480 ±27
No abs.		15943	14555	0.9129 ±0.0023	0.9139	
Al_1	138 126–147	25352	21119	0.8330 ±0.0024	0.8328	639 ±35
No abs.		11479	10412	0.9070 ±0.0038	0.9078	
Al_2	130 114–147	15258	11391	0.7466 ±0.0034	0.7478	666 ±35
No abs.		15281	13848	0.9062 ±0.0023	0.9072	
Cu_1	136 125–147	17926	14986	0.8360 ±0.0027	0.8360	1035 ±62
No abs.		12074	10997	0.9108 ±0.0026	0.9118	
Cu_2	129 110–147	16392	12490	0.7620 ±0.0031	0.7611	1150 ±53
No abs.		14293	13060	0.9137 ±0.0024	0.9147	
Cd_1	135 123–147	24214	20231	0.8355 ±0.0025	0.8355	1651 ±94
No abs.		13638	12416	0.9104 ±0.0025	0.9113	
Sn_1	136 126–147	20815	17693	0.8500 ±0.0030	0.8501	1581 ±115
No abs.		12381	11270	0.9103 ±0.0026	0.9112	
Pb_1	135 122–147	21022	17566	0.8356 ±0.0026	0.8356	2343 ±141
No abs.		7946	7237	0.9108 ±0.0032	0.9115	
Pb_2	126 105–147	13550	10178	0.7511 ±0.0037	0.7503	2622 ±124

[a] Corrected for background.

The experimental data of the measurements with the 122-Mev beam are collected in Table II. Table III gives the data obtained with the 145-Mev beam. In these tables columns 3 and 4 give the total counts of double and quadruple coincidences, respectively. With the 122-Mev beam these counts were obtained in four runs of one minute each with the cyclotron operating at a 12-watt level, while with the 145-Mev beam the counts were obtained in a number of separate runs of 2 minutes each, with the cyclotron operating at a 5-watt level. The ratio Q/D is given in column 5. The stated uncertainty is the larger of either the statistical value or that calculated from the internal consistency. Col-

TABLE IV. Experimental cross sections for negative pions.

Absorber	Experimental cross sections (10^{-27} cm^2) 85 Mev[a]	113 Mev	137 Mev	Geometrical cross section (10^{-27} cm^2) $\pi A^{2/3}(\hbar/\mu c)^2$
C	344± 13	404± 37	414± 27	322
Al	623± 25	655± 54	639± 35	553
Cu	990± 50	1040± 70	1035± 60	977
Cd	1590± 70	1660±130	1650± 90	1430
Sn		1680±140	1580±120	1480
Pb	2400±110	2670±210	2340±140	2150

[a] Data of Chedester, Isaacs, Sachs, and Steinberger, Phys. Rev. **82**, 958 (1951).

umn 6 gives the ratio Q/D after the background corrections have been made. The cross sections computed from these ratios by using (2) were increased by 7±4 percent to account for the muon-electron contamination of the beams, on the assumption that the nuclear interaction of the muons and electrons is negligible, and the resulting experimental cross sections are listed in column 7. The probable error has been increased because of an uncertainty in the background correction, due to the possible variation of the duty cycle of the cyclotron.

Without absorber about 90 percent of the pions which were recorded by the first pair of counters were also recorded by the second pair. Nuclear absorption in the second and third counters and in the lead filter account for 7 percent of the pions. About 1 percent of the pions were lost due to multiple scattering in the second crystal. The remaining 2 percent of the pions were missed due to inefficiency in the last pair of counters.

The experimental cross sections obtained in both beams with the thin absorbers are collected in Table IV. These values have not been corrected for diffraction and Coulomb scattering effects. In this form they are comparable to the values obtained by Steinberger *et al.*,[1] at 85 Mev, which are listed in column 2. For comparison, the geometrical value, $\pi A^{2/3}(\hbar/\mu c)^2$, is listed in column 5. The general result is that all the cross sections have the geometrical value within the accuracy (15 percent) of this experiment. With the possible exception of carbon, the cross sections are independent of energy between 85 and 137 Mev.

The cross sections obtained with the thick absorbers were somewhat larger because of the increase in the contribution of multiple and diffraction scattering effects. For this reason the thick absorber values were not included in Table IV.

TABLE V. Radiation lengths.[a]

Absorber	Radiation length g/cm^2
C	52
Al	26.3
Cu	13.3
Cd	8.9
Sn	8.7
Pb	5.9

[a] From D. J. X. Montgomery, *Cosmic Ray Physics* (Princeton University Press, Princeton, New Jersey, 1949), p. 63.

SCATTERING EFFECTS

The general result, that the nuclear cross sections are close to the geometrical values, suggests that reasonable estimates of the effect of the diffraction scattering might be had from a calculation based on an opaque sphere model.

With this model the result of a partial wave analysis is that, for each partial wave, the total cross section for diffraction scattering is equal to the total cross section for absorption. Using the experimental value for the absorption cross section, σ_a, the differential cross section for the diffraction scattering which includes all partial waves up to $l=l_0$ is

$$\frac{d\sigma_d}{d\Omega}=\frac{\sigma_a}{4\pi(l_0+1)^2}\left|\sum_{l=0}^{l_0}(2l+1)P_l(\cos\theta)\right|^2. \quad (5)$$

For a nucleus of radius $R=A^{1/3}(\hbar/\mu c)$ and a pion of wave number k, the diffraction is calculated by linear interpolation between those adjacent integral values of l_0 most nearly equal to the product kR.

The differential cross section obtained in this way is in reasonable agreement with the results of experiments by Byfield, Kessler, and Lederman[10] and by Isaacs, Sachs, and Steinberger[11] on the elastic scattering of negative pions of energy 62 and 90 Mev by carbon.

The diffraction scattering is predominantly forward and has the effect of spreading the pion beam laterally. The Coulomb scattering also contributes to the lateral spread of the beam. Although the two types of scattering have a different origin, and a different angular distribution, it was considered sufficient for the present purpose to treat both effects together in a simple, if approximate, way. This was done by assuming that the pion beam at the last counter had a Gaussian distribution with total mean square radial displacement $\sum_i\langle r_i^2\rangle_{Av}$ given by the sum of the mean square displacements due to (a) original spread of the beam; (b) spread due to Coulomb scattering; and (c) spread due to diffraction scattering. The fraction of pions not recorded by the last counter is then

$$f=\exp(-R^2/\textstyle\sum_i\langle r_i^2\rangle_{Av}), \quad (6)$$

where R is the effective radius (3.81 cm) of the last counter.

The original spread of the beam is determined by the size of the first two crystals (2.54×2.54 cm^2) and the distance x_1 and x_2 of the crystals No. 1 and No. 2 to the last counter. In the present case,

$$\langle r_0^2\rangle_{Av}=1.08(x_1^2+x_2^2)/(x_1-x_2)^2. \quad (7)$$

[10] Byfield, Kessler, and Lederman, Phys. Rev. **85**, 718 (1952).
[11] Isaacs, Sachs, and Steinberger, Phys. Rev. **85**, 718 (1952).

The spread of the beam due to multiple Coulomb scattering may be calculated from a knowledge of the radiation length in the absorber[9] using the formula

$$\langle r_a^2\rangle_{Av}=(0.0226/\eta^2\beta^2)(\delta n/D_n)x_n^2, \tag{8}$$

where x_n is the distance from the center of the nth scatterer to a point 1 cm inside the last counter and $\delta n/D_n$ is the ratio of the thickness to radiation length of the nth scatterer, η is the momentum of the pions in units of μc, and $\beta=v/c$. The radiation lengths for the absorbers used are listed in Table V.

In the case of the second crystal the spread of the beam due to Coulomb scattering is given by

$$\langle r_c^2\rangle_{Av}=(0.000565/\eta^2\beta^2)x_c^2. \tag{9}$$

For the spread due to diffraction scattering, the fraction of those pions diffracted at angles less than θ_0 was computed for each absorber using the formula

$$g=\frac{2\pi}{\sigma_a}\int_0^{\theta_0}\frac{d\sigma_d}{d\Omega}\sin\theta d\theta. \tag{10}$$

For this fraction the mean square radial displacement at the last counter due to the diffraction in the last absorber alone is given by

$$\langle r_d^2\rangle_{Av}=x_a^2\frac{2\pi}{g\sigma_a}\int_0^{\theta_0}\tan^2\theta\frac{d\sigma_d}{d\Omega}\sin\theta d\theta. \tag{11}$$

TABLE VI. Comparison of thick and thin absorber cross sections in the 145-Mev beam.

Absorber	Absorption and inelastic scattering cross sections (10^{-27} cm^2)
C_1	362± 40
C_2	401± 54
Al_1	582± 50
Al_2	583± 58
Cu_1	978± 76
Cu_2	1080± 72
Pb_1	2262±157
Pb_2	2462±152

Then write

$$\langle r_1^2\rangle_{Av}=\langle r_g^2\rangle_{Av}+\langle r_c^2\rangle_{Av} \tag{12}$$

$$\langle r_2^2\rangle_{Av}=\langle r_1^2\rangle_{Av}+\langle r_a^2\rangle_{Av} \tag{13}$$

$$\langle r_3^2\rangle_{Av}=\langle r_2^2\rangle_{Av}+\langle r_d^2\rangle_{Av}. \tag{14}$$

The fractional acceptance of the last counter with no absorber is proportional to $1-\exp(-R^2/\langle r_1^2\rangle_{Av})$.

In calculating the fractional acceptance with absorber it was assumed that the absorption cross section and the total diffraction cross section have the same value σ. The fraction of pions transmitted by the absorber without being absorbed is $\exp(-\sigma N)$. Of this the fraction $1-\exp(-\sigma N)$ are diffracted and $\exp(-\sigma N)$ are transmitted without being diffracted. The latter have a mean square displacement $\langle r_2^2\rangle_{Av}$ so that the fraction $1-\exp(-R^2/\langle r_2^2\rangle_{Av})$ will be recorded. Of the diffracted pions only $g\,[1-\exp(-R^2/\langle r_3^2\rangle_{Av})]$ will be recorded.

The cross section corrected for spread of the beam effects is obtained by writing instead of (2),

$$\frac{Q/D \text{ with absorber}}{Q/D \text{ without absorber}}=\frac{e^{-\sigma N}\{e^{-\sigma N}[1-\exp(-R^2/\langle r_2^2\rangle_{Av})]+g(1-e^{-\sigma N})[1-\exp(-R^2/\langle r_3^2\rangle_{Av})]\}}{1-\exp(-R^2/\langle r_1^2\rangle_{Av})}. \tag{15}$$

From the data of Bernardini, Booth, and Lederman[2,12] it was estimated that 4±2 percent of the pions were scattered inelastically in the forward direction such that they would give a quadruple coincidence. The cross sections computed using (15) were increased by 11±5 percent to account for the muon-electron contamination of the beams and the inelastically scattered pions which gave quadruple coincidences. The resulting total cross sections for absorption plus inelastic scattering are listed in Table VII.

If the beam were better defined geometrically the effect of the multiple Coulomb scattering would be negligible. In the present experiments it leads to corrections to the cross sections which range from 0 percent (carbon) to 7.5 percent (lead) in the 122-Mev beam and from 0 percent (carbon) to 2.5 percent (26.3 g/cm^2 lead) in the 145-Mev beam. The corrections to the cross sections due to diffraction scattering range from 8 percent (lead) to 20 percent (carbon) in the 122-Mev beam and from 6 percent (13.6 g/cm^2 lead) to 21 percent (5.1 g/cm^2 carbon) in the 145-Mev beam.

In Table VI the cross sections obtained using (15) are listed for the measurements with the 145-Mev beam in which two thicknesses of absorber were used. The cross sections obtained with the thick absorbers are somewhat higher than those obtained with the thin absorbers. This indicates that the spread of the beam

TABLE VII. Absorption plus inelastic scattering cross sections.

Absorber	Absorption + inelastic scattering cross sections (10^{-27} cm^2) 113 Mev	137 Mev	Geometrical cross sections (10^{-27} cm^2) $\pi A^{2/3}(\hbar/\mu c)^2$
C	340± 50	360± 40	322
Al	570± 70	580± 50	553
Cu	940± 90	980± 80	977
Cd	1480±150	1570±110	1430
Sn	1500±160	1510±130	1480
Pb	2350±250	2260±160	2150

[12] Bernardini, Booth, and Lederman, Phys. Rev. **83**, 1277 (1951).

effects have been underestimated. For this reason an uncertainty amounting to 50 percent of the diffraction correction was included in computing the errors listed in Table VII, which lists the cross sections obtained from the thin absorber measurements alone.

The general result is that the nuclear cross sections for absorption plus inelastic scattering of negative pions in the energy range 85 to 137 Mev are close to the geometrical values.

I wish to thank Professor Herbert L. Anderson for his guidance and encouragement throughout this research and Mr. Gaurang B. Yodh for his assistance in conducting the experiment and assembling the equipment.

PHYSICAL REVIEW VOLUME 87, NUMBER 6 SEPTEMBER 15, 1952

Effect of Minority Carriers on the Breakdown of Point Contact Rectifiers

ERNST BILLIG
Research Laboratory, Associated Electrical Industries, Ltd., Aldermaston Court, Aldermaston, Berkshire, England
(Received May 13, 1952)

On the application of short high voltage pulses to point contact rectifiers in the inverse direction thermal instability is observed. Intrinsic conduction due to the thermal generation of electron-hole pairs and the subsequent passage of minority carriers (which are not affected by the potential barrier) is suggested as the cause of electrical breakdown.

IT is well known that the standard barrier layer theory of rectification[1,2] fails to account for the phenomenon of electrical breakdown. Various mechanisms have been suggested to explain the large increase in leakage current observed when the voltage approaches a critical value. As the electrical field in the barrier layer is increased on application of a higher voltage, the following phenomena occur:

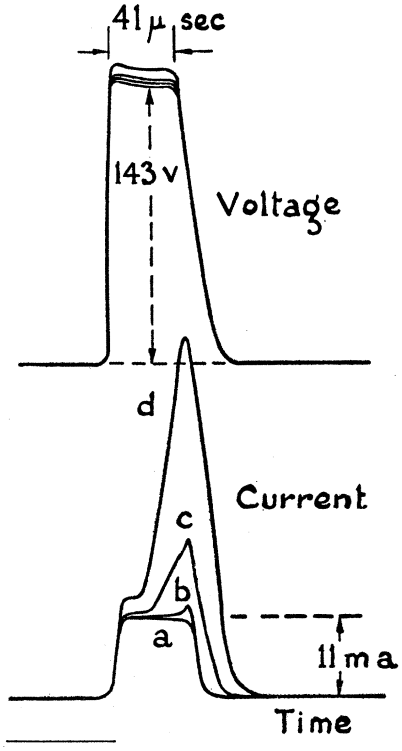

FIG. 1. Thermal instability demonstrated by the application to a Ge point contact diode of constant voltage pulses, with the pulse height increasing from curve *a* to *d*.

1. The image force[3] reduces the effective barrier height greatly easing the passage of carriers from the metal over the barrier into the semiconductor.

2. The barrier becomes sufficiently thin for carriers to tunnel[4] across it. Neither of these mechanisms by itself nor in combination is sufficient to account quantitatively for the experimental observations.

3. The power dissipated in the point contact may raise it locally to a temperature (~150°C in Ge, ~500°C in Si) sufficient for the onset of intrinsic conductivity.[5]

Thermal instability of the barrier layer has recently been shown[6] to account quantitatively for the observed breakdown values in large area (Se) rectifiers. Clear evidence for such instability in point contact rectifiers is given by the cathode-ray oscillogram traced in Fig. 1. Constant voltage pulses[7] of about 40 μsec duration,[8] produced by a low impedance generator, were applied at the rate of 300 per second to a commercial Ge point contact diode (B.T.H. Type CG1) in the inverse direction. Apart from the initial charging peak (not recorded), the current remained constant (curve a). When a certain critical voltage (U_0 = 143 volts) was applied, the current was observed to start rising rather suddenly towards the end of the pulse (curve b). As the voltage was raised only very slightly, the onset of the current

[1] W. Schottky, Z. Physik **118**, 539 (1942).
[2] N. F. Mott, Proc. Roy. Soc. (London) **A171**, 27 (1939).
[3] H. A. Bethe, unpublished MIT Radiation Laboratory Report No. 43-12 (1942).
[4] E. Courant, unpublished Cornell University report (1943).
[5] S. Benzer, J. Appl. Phys. **20**, 804 (1949).
[6] E. Billig, Proc. Roy. Soc. (London) **A207**, 156 (1951).
[7] This was first demonstrated by the author during a lecture on "The Physics of Transistors" given before the Institute of Physics in London on 18th March, 1952. I am indebted to Mr. M. S. Ridout for taking these oscillograms for me.
[8] Considerably shorter pulses (<1 μsec) have been used by Bennett and Hunter (Phys. Rev. **81**, 152 (1951)). The much higher voltage that contact rectifiers can withstand for such short times is in perfect agreement with the postulate of thermal instability (see reference 6).